Pc 1 waves and associated unstable distributions of magnetospheric protons observed during a solar wind pressure pulse

R. L. Arnoldy,[1] M. J. Engebretson,[2] R. E. Denton,[3] J. L. Posch,[2] M. R. Lessard,[1] N. C. Maynard,[4] D. M. Ober,[4] C. J. Farrugia,[1] C. T. Russell,[5] J. D. Scudder,[6] R. B. Torbert,[1] S.-H. Chen,[7] and T. E. Moore[7]

Received 1 February 2005; revised 5 April 2005; accepted 9 May 2005; published 28 July 2005.

[1] We present observations of Pc 1 waves (~0.6 Hz) that occurred shortly after a strong (>20 nPa) compression of Earth's magnetosphere at 1321 UT, 18 March 2002. Intense Pc 1 waves were observed at several high-latitude ground stations in Antarctica and Greenland from 1321 UT to beyond 1445 UT. Two wave bursts were recorded at the Polar satellite at 1338 and 1343–1344 UT as it passed outbound in the Southern Hemisphere at 1154 local time (SM magnetic latitude of −22° and near L = 7.5) in good magnetic conjunction with the Antarctic. The pressure increase created a significant population of protons between a few hundred eV and several keV, whose fluxes were mostly perpendicular to B. These protons seem to have replaced the quiescent stream of protons (presumably convected from the plasma sheet) that existed before this increase. There was also a nearly two-order-of-magnitude increase in the population of thermal/suprathermal (0.32–410 eV) protons. The generation of ion cyclotron waves is expected to limit the proton temperature anisotropy A, defined as $T_\perp/T_\parallel - 1$. The ion cyclotron instability driven by the observed hot ion temperature anisotropy is studied using two models, with and without the presence of cold background plasma. Peaks in the calculated instability as a function of time show excellent agreement with the times of the Polar wave bursts, which were measured a few tens of seconds after maxima in the instability calculation. The time delay is consistent with the propagation time to the spacecraft from a source nearer to the equatorial plane. The hot proton population at Polar appears to be driven back to stability by a sudden increase in very field-aligned protons having energies less than the hot perpendicular population, suggesting a different source for the two populations. These observations confirm the importance of both the energization and/or increase in population of protons transverse to B in the several keV range (possibly betatron acceleration as a result of the pressure pulse), and the presence of greatly increased fluxes of lower energy protons (100s of eV to a few keV), predominantly aligned along B, in determining whether the particle population is unstable at a given time.

Citation: Arnoldy, R. L., et al. (2005), Pc 1 waves and associated unstable distributions of magnetospheric protons observed during a solar wind pressure pulse, *J. Geophys. Res.*, *110*, A07229, doi:10.1029/2005JA011041.

1. Introduction

[2] The predominant high-latitude (L = 6–8) ground ULF signal near local noon is quasi-structured hydromagnetic chorus/emissions [*Fukunishi et al.*, 1981; *Menk et al.*, 1993; *Anderson et al.*, 1995]. Since the early 1960s, it has been noted that the ULF waves on the ground near local noon were either turned on or enhanced in association with sudden impulses in the Earth's magnetic field [*Troitskaya*, 1961; *Heacock and Hessler*, 1965; *Kokubun and Oguti*, 1968; *Troitskaya et al.*, 1968; *Hirasawa*, 1981]. Early in situ solar wind measurements have related these sudden magnetic impulses with pressure pulses in the solar wind plasma which would compress the magnetosphere and could drive the trapped proton radiation unstable to EMIC wave growth, as suggested by *Olson and Lee* [1983]. An analysis of the

[1]Space Science Center, University of New Hampshire, Durham, New Hampshire, USA.
[2]Department of Physics, Augsburg College, Minneapolis, Minnesota, USA.
[3]Department of Physics, Dartmouth College, Hanover, New Hampshire, USA.
[4]ATK Mission Research, Nashua, New Hampshire, USA.
[5]Institute of Geophysics and Planetary Physics, University of California, Los Angeles, California, USA.
[6]Department of Physics, University of Iowa, Iowa City, Iowa, USA.
[7]NASA Goddard Space Flight Center, Greenbelt, Maryland, USA.

0148-0227/05/2005JA011041$09.00

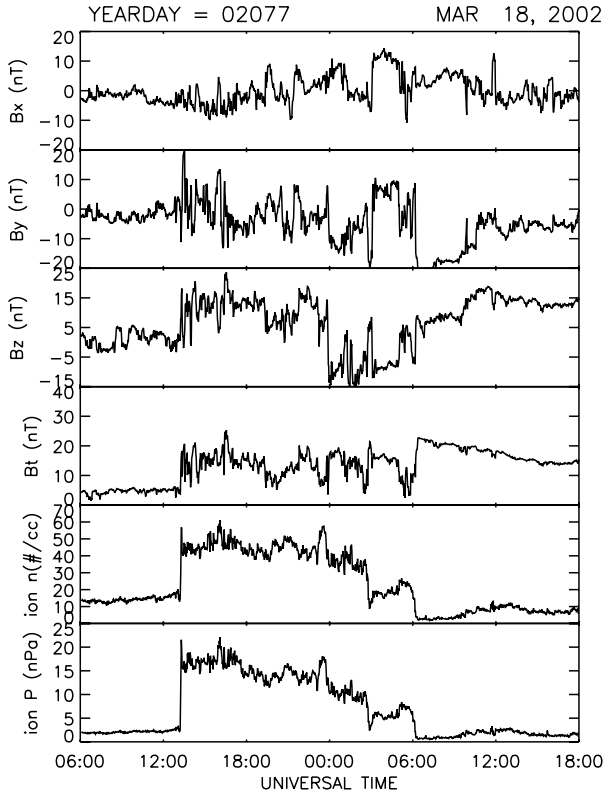

Figure 1. Interplanetary parameters measured by the Wind spacecraft. The magnetic field is in GSM coordinates.

particle and field data from the AMPTE/CCE satellite in the outer, dayside, equatorial magnetosphere during magnetospheric compressions indeed suggest that enhancements in dynamic pressure drive the energetic proton distributions trapped in the outer magnetosphere to instability producing the EMIC waves measured by the spacecraft [*Anderson and Hamilton*, 1993]. No correlation of spacecraft waves with ground measurements was made in this study. However, *Anderson et al.* [1996a] have related AMPTE/CCE equatorial waves with ground ULF waves rather convincingly but at this time the particle measurements were not available to determine the particle instability to wave generation during the compression events. This work has shown that the space wave bursts above the He^+ gyrofrequency reached the ground implying that the H^+-He^+ bi-ion resonance did not prevent this from happening in this case.

[3] Recently, a general correlation of Pc1 waves (0.2–5 Hz) measured on the ground and ULF waves measured in space has been made with proton populations in the outer dayside magnetosphere [*Engebretson et al.*, 2002]; however, no stability analysis of the particles could be made in this study because the satellite observations were made at midlatitudes, far from the presumed equatorial source of the waves. A similar study of ground Pc1-2 waves that presumably map poleward of the dayside cusp with satellite wave and particle data has also been made (M. J. Engebretson et al., Ground and satellite observations of Pc1-2 waves on open field lines poleward of the dayside cusp, submitted to *Journal of Geophysical Research*, 2005). Quantitative estimates of the ion cyclotron instability of the observed ion distributions were found to be stable at the altitudes traversed by the Polar satellite but might reasonably be inferred to be unstable in the exterior mantle, a location consistent with their observed wave frequency. There has been much work recently to correlate ground ULF wave data with spacecraft wave measurements, particularly, the highly structured Pc 1 Pearl Events [*Erlandson et al.*, 1994; *Erlandson et al.*, 1996; *Mursula et al.*, 1997; *Bräysy and Mursula*, 2001; *Guglielmi et al.*, 2001; *Mursula et al.*, 2001]. This work has cast considerable doubt on the validity of the bouncing wave packet model for the structure of the Pearl events and provides additional motivation for looking directly at the particles responsible for the waves. A very early model for the structure of Pc 1 Pearls focused on a bouncing, slow proton bunch [*Jacobs and Watanabe*, 1963]. Such proton bunching has been measured at geosynchronous orbit [*Quinn and Southwood*, 1982] attributed to transient Earthward convection surges in the magnetosphere. Recently, intermittent ion injections have been measured in the dayside magnetosphere during pressure pulses suggesting intermittent magnetic reconnection at the high-latitude magnetopause as a consequence of compressional waves produced by the solar wind dynamic pressure [*Lu et al.*, 2004]. This study represents an attempt to correlate ground ULF signals with particle populations in space that can be shown to be unstable to wave growth and thereby be a source of the ground waves.

2. Event

[4] The dynamic pressure of the solar wind never exceeded several nPa for a period of time from 5 March 2002 to 18 March 2002. On 18 March 2002 the pressure rose abruptly to over 20 nPa as measured at the Wind spacecraft located near apogee of its petal Orbit (X = 44 R_E, Y = −122 R_E, and Z = −4 R_E in GSE coordinates). The pressure remained above 5 nPa from the time of its onset at 1315 UT, 18 March, to a time of sudden release at 0600 UT on 19 March. From the time of the pressure onset the Bz component of the interplanetary magnetic field remained essentially positive until the start of 19 March when there were several negative Bz excursions. These interplanetary parameters are summarized in Figure 1. The solar wind plasma data were obtained by the Solar Wind Experiment on the Wind spacecraft [*Ogilvie et al.*, 1995] and the interplanetary magnetic field data obtained by the Magnetic Field Instrument on Wind [*Lepping et al.*, 1995]. These data were accessed using the CDAWEB facility (http://cdaweb.gsfc.nasa.gov) at NASA Goddard Space Flight Center.

[5] At the time of the pressure pulse, the Polar spacecraft was in the Southern Hemisphere at −22° magnetic latitude and a magnetic local time of about 1130 moving toward the equatorial plane and the magnetopause. The model [*Tsyganenko*, 1989] (Kp = 3.3) projected footprint of Polar on Antarctica (Figure 2) brings the spacecraft within a few to several degrees of the British Antarctic Survey Automated Geophysical Observatories A80 and A81 at various times between 1320 UT and 1400 UT. Figure 2 also shows the location of BAS station A84 and South Pole Station (SP) in the Antarctic and the projection of Sondrestromfjord (SS) located in Greenland since data from all these sites will be presented in this paper. The geographic and geomagnetic coordinates of these stations are listed in Table 1. Multi-

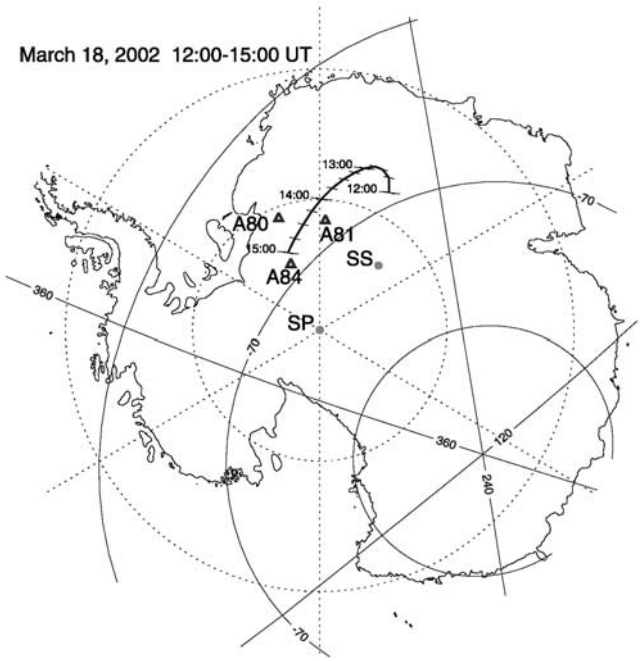

Figure 2. Projection of the Polar spacecraft trajectory onto Antarctica using the Tsyganenko 1989 (Kp = 3.3) model.

instrument Automated Geophysical Observatories (AGOs) in Antarctica operated by the United States [*Rosenberg and Doolittle*, 1994] and United Kingdom [*Dudeney et al.*, 1997] include search coil magnetometers, which provide vector samples of dB/dt each 0.5 s in local geomagnetic coordinates with X northward and Y eastward [*Taylor et al.*, 1975; *Engebretson et al.*, 1997]. Similar search coil magnetometers at South Pole Station, Antarctica and Sondrestromfjord, Greenland, provide vector samples each 0.1 s.

[6] This study will use data from four Polar spacecraft instruments. Observations of ULF waves on Polar are obtained by the Magnetic Fields Experiment [*Russell et al.*, 1995], which samples the ambient vector magnetic field at 0.12-s intervals. The Hydra spectrometer on Polar [*Scudder et al.*, 1995] samples 3-D distributions of electrons and ions (assuming H^+) over the energy range from ~10 eV to 19 keV. The distribution functions used in this study have a temporal resolution of 13.8 s. These 13.8-s distributions are averages of the ion and electron energy sweeps made over the entire energy range in 1.15 s. The Electric Field Instrument on Polar [*Harvey et al.*, 1995] determines vector electric fields at 0.05-s intervals by means of three orthogonal pairs of booms with tip-to-tip separations of 100 m and 130 m (in the spin plane) and 13.8 m (along the spin axis). Finally, the TIDE instrument measured the thermal/superthermal ion population from 0.32 to 410.62 eV [*Moore et al.*, 1995].

Table 1. Locations of the Ground Stations Used in This Study

	Geographic		Geomagnetic	
Site	Lat	Long	Lat	Long
A80	80.7 S	20.4 W	66.5 S	28.5 E
A81	81.5 S	3.0 E	68.9 S	35.8 E
A84	84.4 S	23.9 W	68.9 S	25.7 E
South Pole	90 S	–	74.0 S	18.4 E
Sondrestromfjord	67.0 N	309.3 E	74.2 N	42.8 E

[7] The impact of the interplanetary pressure pulse on the Earth's magnetic field is evident in Figure 3, which shows the difference between the vector magnetic field observed by the UCLA Magnetic Field Instrument aboard Polar and the IGRF model. The Earth's field is compressed with the X component reduced by about 50 nT and the Z component increased 140 nT. There is no evidence of Polar leaving the magnetosphere until after 1400 UT.

[8] The effect of this compression on the magnetospheric particle population as measured by the University of Iowa HYDRA experiment is summarized in Figure 4. The top panel is a differential energy ion spectrogram over all pitch angles and energies above a few tens of eV, similar to the second panel which is the same but for electrons. The bottom three panels limit the ion spectrograms to pitch angles representative of parallel, transverse, and antiparallel to B directions. The pressure pulse is evident in the particles as a sudden change in their spectrograms from familiar magnetospheric distributions before 1322 UT to generally accelerated/intensified populations. The ring current protons, at the highest energy measured, are accelerated and perhaps intensified as a result of the pressure pulse. The same is true for the stream of protons around a few keV,

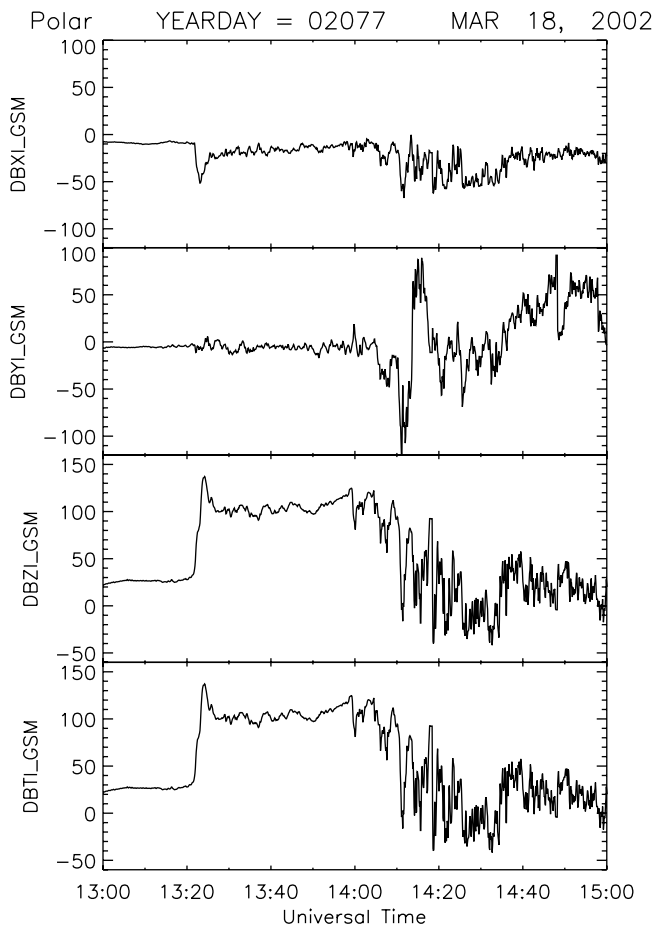

Figure 3. Differences between the Polar measured magnetic field and the IGRF model in GSM coordinates.

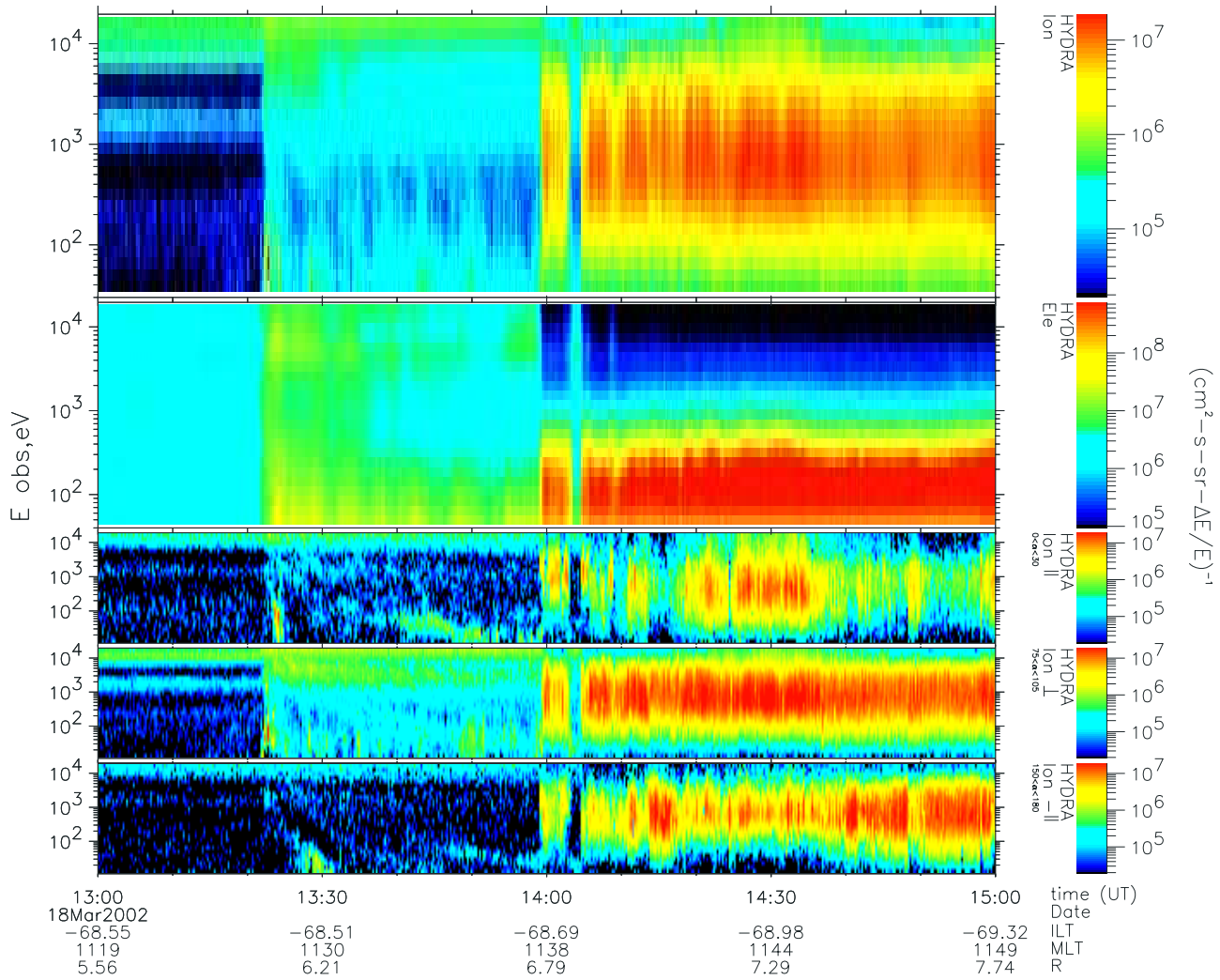

Figure 4. Particle spectrograms measured by the Polar Hydra instrument. The top panel is a differential energy ion spectrogram over all pitch angles and energies above a few tens of eV, similar to the second panel which is the same but for electrons. The bottom three panels limit the ion spectrograms to pitch angles representative of parallel, transverse, and antiparallel to B directions.

presumably plasma sheet protons, except to a higher degree at pitch angles transverse to B. An impulsive injection of protons with increasing energy dispersion is quite evident in the antiparallel population and somewhat less so in the parallel protons, quite similar to the event discussed recently by *Lu et al.* [2004] resulting from a pressure pulse. The *Lu et al.* [2004] paper suggests these ions are transported into the magnetosphere as a result of intermittent, high-latitude reconnection. Another boundary is crossed at about 1400 UT when Polar seems to have entered the magnetosheath displaced inward by the pressure pulse.

[9] It appears that the region from 1320 to 1400 UT is not a typical boundary layer region with just a mixture of magnetospheric and magnetosheath particles but new populations are evident in both the electrons and ions presumably as a result of the pressure pulse. If reconnection is important, it would have to have taken place at high latitudes (poleward of the cusp), since Bz was predominantly positive in the solar wind during this time. The accelerated and intensified protons measured uniquely perpendicular to B will be our primary interest in this paper, since we are interested in the source of ULF waves measured both in space and on the ground resulting from the pressure pulse.

3. Polar and Ground ULF Waves

[10] Figure 5 gives frequency versus time spectrograms of the north-south (X) component of the induction ground magnetometer data obtained from the five sites shown in Figure 2. SP and SS were sampled at 10 Hz as compared with just 2 Hz for the BAS sites (A80, A81, and A84); hence there is data not shown for SP and SS that goes up to 5 Hz. Data missing for these two sites in Figure 5 is that the Pi 1 burst at the time of the impact of the solar wind pressure pulse extended up to about 3 Hz. The signals between 0.25 and 1.0 Hz are the noon sector quasi-structured chorus emissions classified by *Fukunishi et al.* [1981]. South Pole at higher latitude than the BAS stations sees weak chorus while Sondrestromfjord, also at a higher

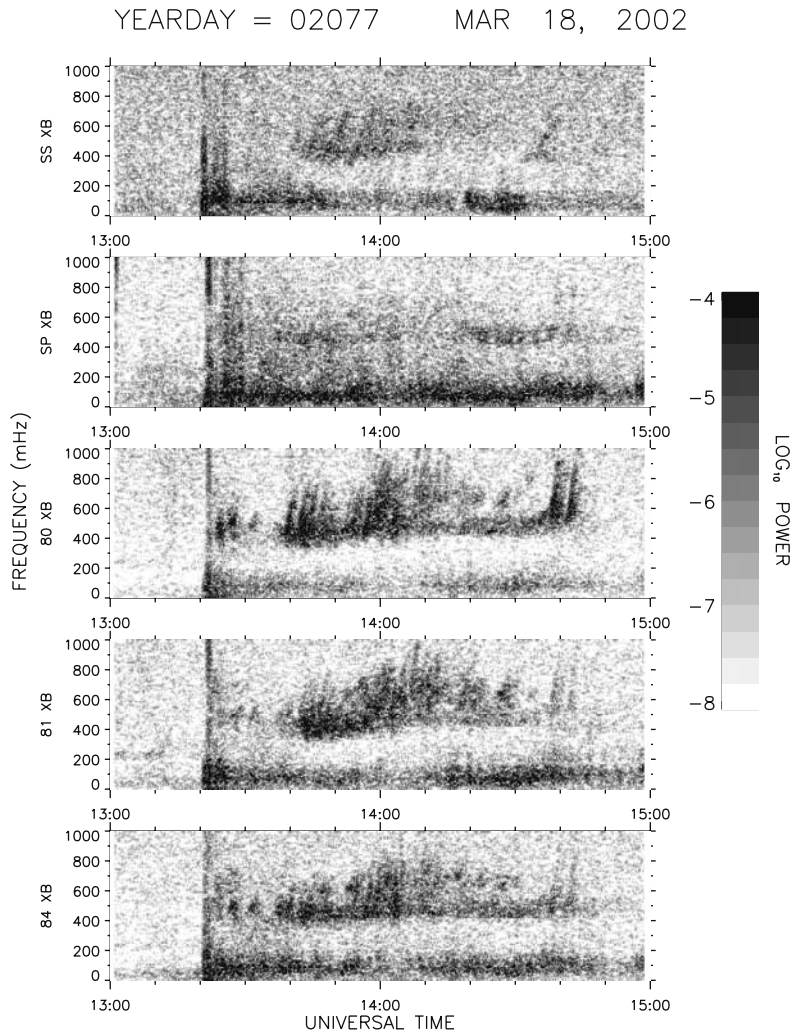

Figure 5. Frequency versus time spectrograms using the north-south (X) component of the induction ground magnetometer data obtained from the five sites shown in Figure 2 and listed in Table 1.

latitude than the BAS stations, sees more chorus but generally of different structure.

[11] Figure 6 gives frequency versus time spectrograms of the two transverse components of the Polar magnetic field data (field-aligned coordinates with Y magnetically eastward and X radially outward) and the X component (north-south) of the ground site A80 for the hour 1300–1400 UT. This was the time when the spacecraft was measuring the particle population of the quiescent magnetosphere followed by a period of compressed field and accelerated/intensified particle populations commencing at 1322 UT, as discussed above. Figure 6 also gives the ellipticity of the Polar and ground data where −1 is left circular polarization and +1 right in panels 3 and 5. At about 1358 UT, when Polar entered the magnetosheath, intense broadband waves were measured. In the early several minutes of the compression at 1322 UT, Figure 6 also shows the existence of a mixture of broadband waves similar to those measured in the magnetosheath and narrowband bursts of waves less than a few Hertz, similar to what has been reported by *Song et al.* [1990] and *Anderson and Fuselier* [1993] and reviewed by *Tsurutani et al.* [2003]. It is not known whether the narrowband bursts of ULF waves above 1 Hz seen by Polar in the first several minutes after the pressure pulse were seen on the ground at the stations most conjugate to Polar (the BAS stations), since these stations did not measure above 1 Hz. Clearly, they were not seen at the more distant sites SP and SS where measurements were made up to 5 Hz.

[12] In comparing Polar waves near 0.5 Hz with those on the ground at BAS station A80 in Figure 6, it is not clear whether the ground sites were measuring the same waves as the Polar magnetometer. One conclusion is evident in that the ground signals are considerably more structured. The sloping structures to the right might be due to the slower propagation speed at the higher frequencies, although even in the segment of data shown there appear to be non-dispersed signals just ahead of 1330 UT. There is no question that the ground signals take a very tortuous path to get to the ground antennas, presumably horizontal ducting and then leaking out of this duct to get to the ground explaining why the different stations can see differ-

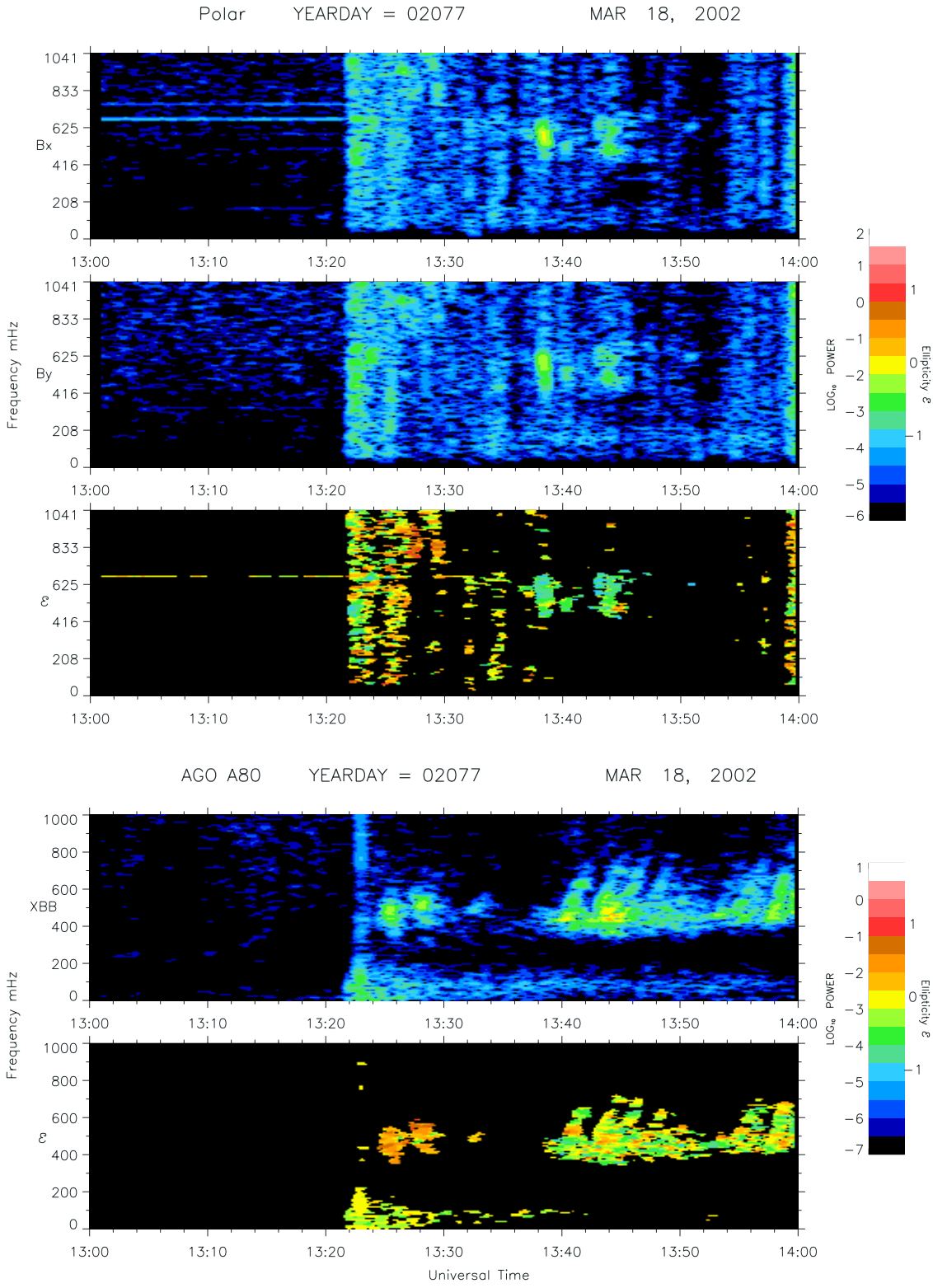

Figure 6. Frequency versus time spectrograms of the two transverse components of the Polar magnetic field data (field-aligned coordinates with Y magnetically eastward and X radially outward in the top two panels) and the X component (north-south) of the ground site A80 in the fourth panel from the top. Panels three and five (bottom) give the ellipticity of the Polar and ground data respectively where −1 is left circular polarization and +1 right.

ent structure as is evident in Figure 5. The polarization of the 0–1 Hz Polar signals between 1300 and 1400 UT, given in the third panel of Figure 6, shows that the ULF bursts between 1338 and 1345 UT clearly have an ellipticity near −1 or are left-handed waves. The bottom panel gives the ellipticity of the ground signals showing generally a mixture of polarization with a suggestion of right polarization ahead of 1330 UT. Such a mixture of ground ULF waves is not unexpected since ground sensors could detect leakage of both Alfven and fast waves out of the ionospheric duct. Note that just after the pressure pulse at 1322 UT, the Polar signals also have a mixture of polarization.

[13] For the most intense burst of ULF waves less than 1 Hz measured at Polar at 1338 UT, we have combined the Polar B field with the Polar electric field [*Harvey et al.*, 1995] to calculate the Poynting vector in a FA coordinate system. Figure 7 gives in the top three panels the B field in GSM coordinates and the bottom three panels are the electric field in the same coordinate system. The B field in the FAC coordinate system is given in the fourth panel from the top and the Poynting vector in the same coordinate system is given in the fifth panel from the top. Clearly, these ULF waves at Polar are propagating antiparallel to the magnetic field toward the Southern Hemisphere.

4. Ion Cyclotron Instability of Observed Ion Distributions

[14] In studies of the Earth's ring current and its decay there has been considerable work on the generation of EMIC waves by energetic ions in the inner magnetosphere near the plasmapause [*Thorne and Horne*, 1994; *Kozyra et al.*, 1997; *Thorne and Horne*, 1997; *Jordanova et al.*, 2001]. This section will focus on the Polar particle populations to see whether the instability theory driven by proton temperature anisotropy at geosynchronous orbit [*Gary et al.*, 1994; *Gary et al.*, 1995] and near the magnetopause [*Anderson et al.*, 1996b] can also characterize the source of the ULF waves measured by the Polar magnetometer for this event at L = 7.5. Utilizing both the hot and cold protons measured aboard the Polar spacecraft a condition according to *Gary et al.* [1994] for this instability is

$$A\left(\beta_{\|\,h}\right)^{0.44}(n_c/n_h)^{0.25} \geq 0.5 \qquad (1)$$

where the temperature anisotropy (defined as $A = T_\perp/T_\| - 1$) for our study uses the temperatures of the Maxwellian fit to the energetic protons between 0.1 and 10 keV measured by the Polar Hydra instrument parallel and perpendicular to the magnetic field and $\beta_{\|\ h}$ is the parallel plasma beta (defined as $8\pi n_h k T_\|/B^2$). The hot density, n_h, is the zeroth moment over the entire energy range of the Hydra protons and the number density of the cold plasma, n_c, is that measured by the Tide instrument over the energy range 0.32 to 410.62 eV. However, concerned about the effect spacecraft charging might have on the measurement of thermal particles, *Gary et al.* [1995] found that an upper bound on the hot proton anisotropy which was independent of the ratio of hot to cold densities provided a "more robust" basis for comparison against observations. This condition for instability:

$$A\left(\beta_{\|h}\right)^{0.47} \geq 0.39 \qquad (2)$$

is a form of equation (4) in the work of *Gary et al.* [1995].

[15] Figure 8a gives the integrated power of the waves greater than 0.4 Hz measured by the Polar magnetometer, shown earlier in Figure 6 in spectrogram form. Of interest here will be the two bursts of power between 1338 and 1345 UT, which correspond to the two bursts of narrowband waves in Figure 6. Figures 8c and 8d give the measured proton temperatures perpendicular and parallel to B, respectively, as obtained from the Polar HYDRA data between 100 eV and 10 keV energy. Figure 8b gives the results of the instability calculations using both equation (1) (solid line) and equation (2) (dashed line). Figure 8e gives the TIDE cold density used in equation (1). The instability curve obtained from equation (2) never quite exceeds 0.39, suggesting that the hot protons are not locally unstable to EMIC wave growth, while the instability calculated from equation (1) often exceeds the threshold of 0.5. Perhaps one reason why equation (1) gives excessively large values is that the measured ratio of hot to cold densities during this event is a factor of 4 lower than the minimum value of the range that *Gary et al.* [1994] specified for the validity of their equation. It is apparent, however, that there are two enhancements of the calculated "instability" at about 1338 and 1344 UT.

[16] Figure 8d is interesting in that the parallel temperature of the energetic Hydra protons appears to be anticorrelated with the instability curves of the second panel. Figure 9 gives three sample contour plots of the logarithm of the distribution function (f) of the Hydra protons plotted against $v_\perp$ and $v_\|$. The three plots span the period of time when the intense Polar ULF waves were measured by the magnetometer at 1338 UT. All three panels show the transverse heating from a few hundred eV to over 5 keV (1000 km/s) presumably due to the compression of the Earth's magnetic field by the solar wind pressure pulse. The panels at 1335:05 and 1338:46 show also that there is a heated parallel/antiparallel proton population from a few hundred eV but extending only up to about 2 keV (about 600 km/s) which correlates with the reduction in the calculated instability of Figure 8 at these times. Both of these populations appear to play a very significant role in the generation of ULF waves driven by the temperature anisotropy of the proton population. An earlier study of ULF waves and magnetospheric protons [*Engebretson et al.*, 2002] has also pointed to protons in this energy range as appearing to be the origin of ULF waves in space and on the ground.

[17] A further comment is in order about the anticorrelation of the HYDRA Proton Instability plot of Figure 8b and the Parallel Temperature of Figure 8d. Perhaps stated another way, the instability of the plasma is decreased when the streaming of protons of a few KeV energy along B is enhanced which reduces the anisotropy of the transverse protons. These protons are seen in Figure 4 (third and fifth panels from the top) as the energy dispersed structures. Using the dispersion seen in the antiparallel protons

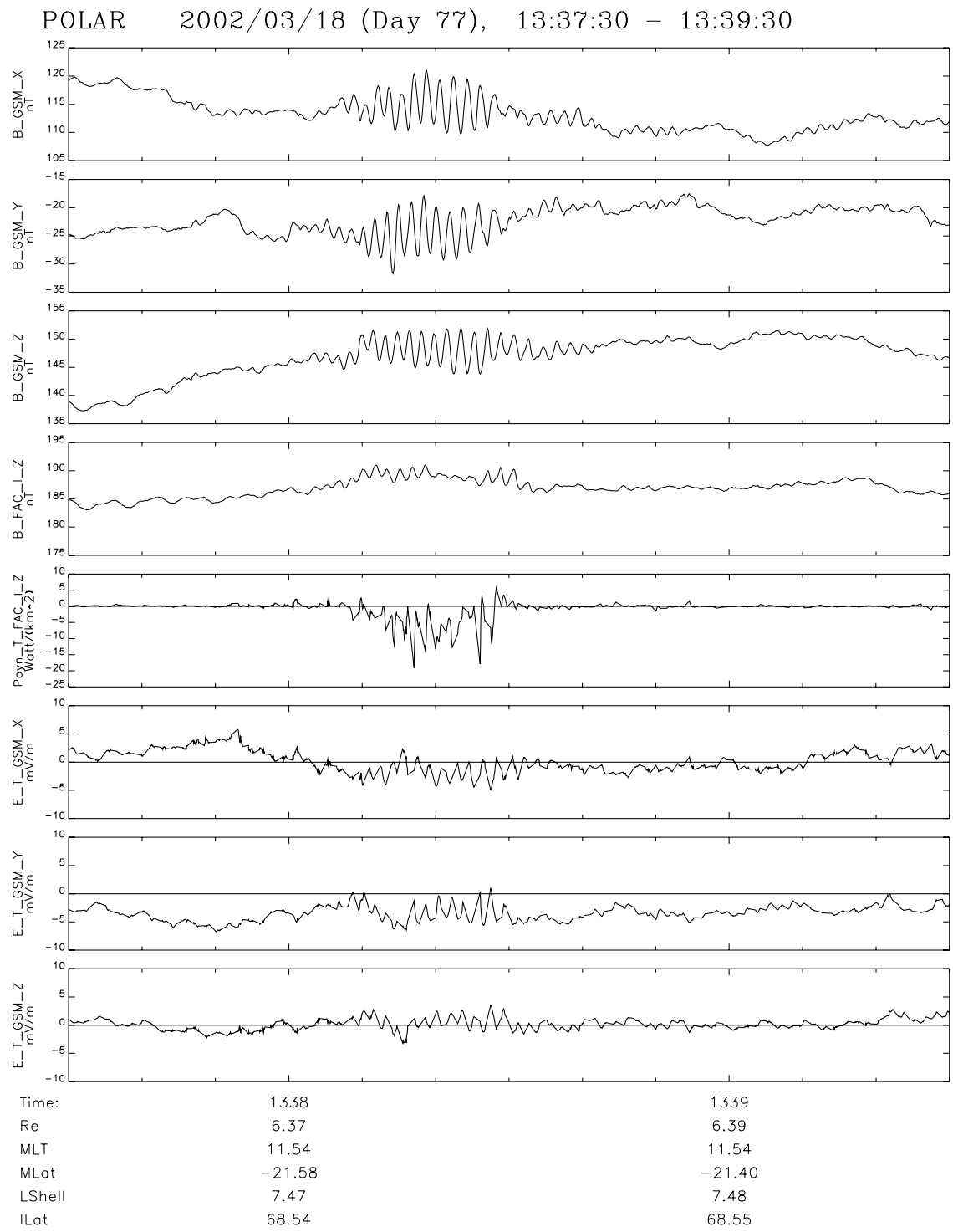

Figure 7. Polar magnetic field data in GSM coordinates in top three panels. Polar electric field data also in GSM coordinates in bottom three panels. Total magnetic field in field-aligned coordinates in fourth panel from the top and the Poynting vector in the fifth panel from the top (postive direction is along B).

assuming that all energies originated in one region along B, one gets a source of these particles at very high latitudes near the northern cusp.

[18] For the two peaks in ''instability'' in Figure 8, it is apparent that there is a slight lag of a few tens of seconds in Polar integrated ULF power as compared with the calculated ''instability'' of the Polar proton population, indeed suggesting that the wave power measured may not have been generated at the location of Polar but propagated to the spacecraft from another source or sources. This would be consistent with the fact that the use of (2) does not result in a local instability. The observed 30 ± 15 s delay between the times of peaks in local instability and the times waves appear is consistent with the strongly unidirectional nature

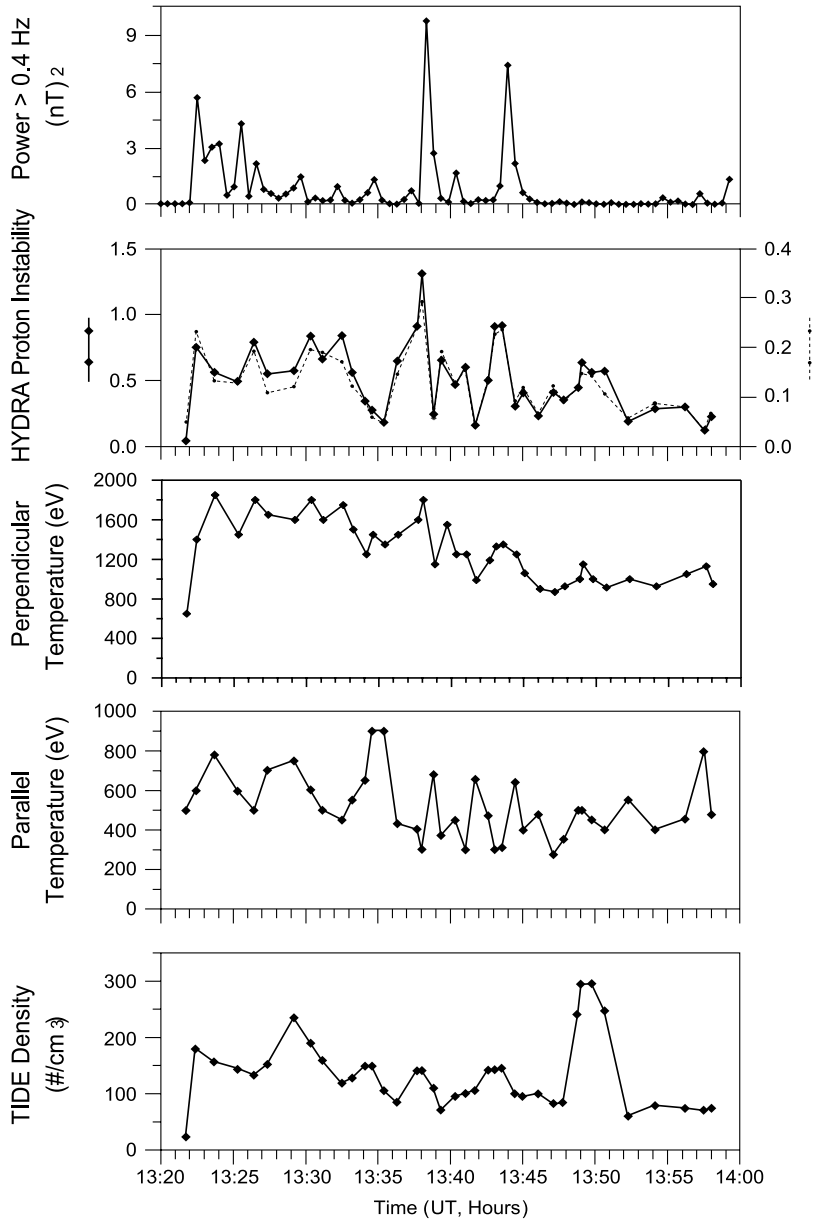

Figure 8. Top panel: Integrated ULF wave power measured by Polar above 0.4 Hz. Second panel: Solid line is an instability calculation using equation (1) and the dashed line from a revision of this equation [*Gary et al.*, 1995] eliminating the direct dependence on the ratio of hot to cold proton densities (equation (2)). Third panel: Maxwellian perpendicular temperature of Hydra protons between 0.1 keV and 10 keV. Fourth panel: Maxwellian temperature of Hydra protons between 0.1 keV and 10 keV moving along or antiparallel to B. Bottom panel: Measured density of protons measured by the TIDE detector having energies between 0.32 and 410.62 eV.

of the Poynting flux (toward the ionosphere) in suggesting that the waves observed by Polar were not generated locally, at $-21.5°$ GMLAT for the event at 1338 UT and at $-20.6°$ GMLAT for the event at 1344 UT but rather on the same flux tube closer to the magnetic equator.

[19] One must keep in mind that the agreement found here between the calculation of instability of the proton population and the measured ULF waves aboard Polar does not necessarily assure that only protons on the field line through Polar are solely the source of the measured ULF waves, since waves above the equatorial He^+ gyrofrequency are loosely tied to the generation field line. Furthermore, the very complex ground ULF waves in Figure 5 could originate from sources on several field lines and at different latitudes since the propagation to the ground sensor is not well-defined.

[20] In the following section we present quantitative estimates of the location in latitude where the first wave burst originated, based on the above time delay. Our procedure involves numerically estimating the time needed for Alfven waves to reach the satellite's location at 1338 UT from various latitudes of origin and comparing that to the

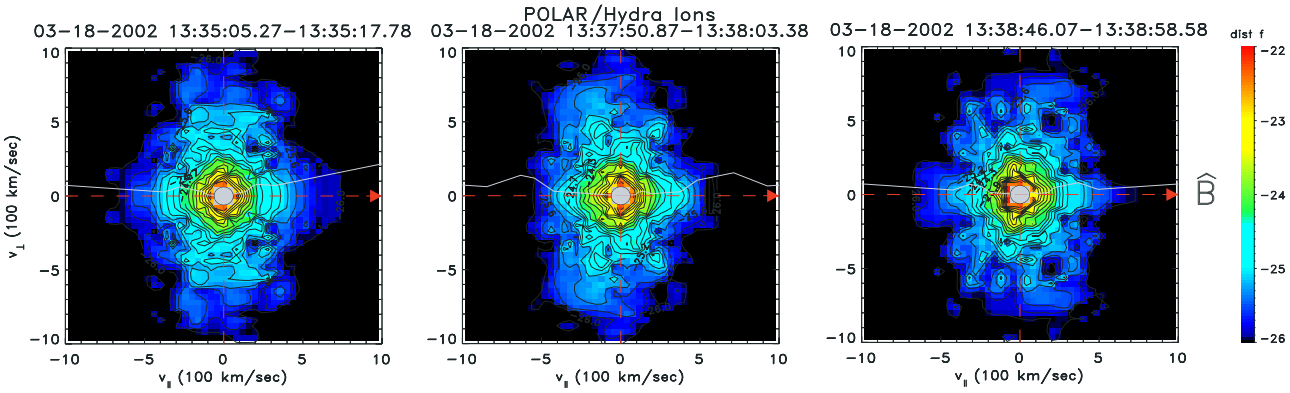

Figure 9. Phase space plots of the proton distribution function (color scale) for times bracketing the large ULF wave burst at 1338 UT showing how the parallel component of the population damps the instability resulting from the very hot perpendicular population greater than 100 eV energy created by the large solar wind pressure pulse (compare with the plots of Figure 8).

estimated travel time of representative 1 keV and 500 eV field-aligned ions associated with the time of maximum instability. (Incorporating a latitude-dependent parallel ion velocity is not necessary for nearly field-aligned ions but is necessary for those ions that have large pitch angles away from the equator. For the purposes of this estimate, however, we have not performed this much more complex calculation.)

[21] At this time the magnetic equator was 15° south of the Earth-Sun line, so one might naively expect the greatest impact of the interplanetary shock that caused the magnetospheric compression, and hence the probable location of wave origin, to be at or northward of the magnetic equator. Indeed, calculation of the shock normal vector using ACE magnetic field data gave direction cosines of (0.806, 0.243, 0.540) in the GSM coordinate system. That is, the normal to the shock plane was directed earthward at an angle ~34° southward of the Sun-Earth line, resulting in the first impact of the shock occurring considerably northward of the geomagnetic equator.

[22] Using the observed magnetic field magnitude at 1338 UT, **B** = 188 nT, and its radius from Earth, 6.4 R_E, along with the *Tsyganenko and Stern* [1996] field model (but adjusted to the observed total field at this location), and assuming an electron (and ion) density of 150 cm^{-3}, we determined **B** at locations every 0.03 R_E along this model field line.

[23] Calculation of the wave travel time also requires knowledge of three additional quantities: the proportion of heavy ions, the ratio of the observed wave frequency to the local proton gyrofrequency (necessary to infer the group velocity), and the density at each point along the field line.

[24] Table 2 lists the nine cases examined. Case 1 assumes a "typical" ion composition ratio, with 94% H^+, 5% He^+, and 1% O^+. The He^+ density was changed by factors of 2 in cases 2 and 3, and the O^+ density was changed by these same factors in cases 4 and 5. Cases 6 and 7 involve different profiles of density along the field line, and cases 8 and 9 change the total ion density by factors of 2.

[25] The observed wave frequency of 0.573 Hz was 20% of the local proton gyrofrequency, so the wave was on the He^+ cyclotron surface (a left-handed surface which approaches the helium gyrofrequency at large wave vector $k_{||}$). Using the dispersion relation (2) in the work of *Summers and Thorne* [2003] for parallel propagation of left-handed electromagnetic ion cyclotron waves in cold plasma, the group velocity was calculated using the modeled ion density, magnetic field, and ratio of wave frequency to proton gyrofrequency. The resulting group velocities were considerably lower than the Alfven speed because the waves were close to the He^+ resonance. For example, at 1338 UT the local Alfven velocity was 305 km/s, but the group velocity, calculated using the several assumed concentrations of He^+ and O^+ listed in Table 2, ranged from 160 km/s down to 80 km/s.

[26] The mass density profile used was based on the well-known power law formula

$$\rho = \rho_{eq}(R_{Max}/R)^{\alpha} \quad (3)$$

where ρ_{eq} is the equatorial mass density, and R_{Max} is the maximum distance to any point on the field line, and hence ~L * R_E [*Denton et al.*, 2002]. For this calculation, the local electron density (150 cm^{-3}) and α are used to calculate ρ_{eq}.

[27] *Denton et al.* [2002] determined α to be in the range 1.6–2.1 in the plasmatrough ($L \geq 7$), but with α closer to 1 or even less in the 0900–1500 MLT sector and L beyond 6 (up to 8). *Denton et al.* [2002] noted that a similar average

Table 2. Ion Density Models Used in Time Delay Calculations[a]

Case	α	η_H	η_{He}	η_O	χ	v_g
1	0	0.94	0.05	0.01	1.0	112
2	0	0.89	0.10	0.01	1.0	80
3	0	0.965	0.025	0.01	1.0	149
4	0	0.93	0.05	0.02	1.0	110
5.	0	0.945	0.05	0.005	1.0	112
6	2	0.94	0.05	0.01	1.0	103
7	−1	0.94	0.05	0.01	1.0	116
8	0	0.94	0.05	0.01	0.5	158
9	0	0.94	0.05	0.01	2.0	79

[a]The radial density power law coefficient α is defined in (3), and η_H, η_{He}, and η_O are composition fractions (with sum = 1.0). The electron density at the spacecraft is given by χ * (150 cm^{-3}). The last column indicates the group velocity at the spacecraft position, in km/s.

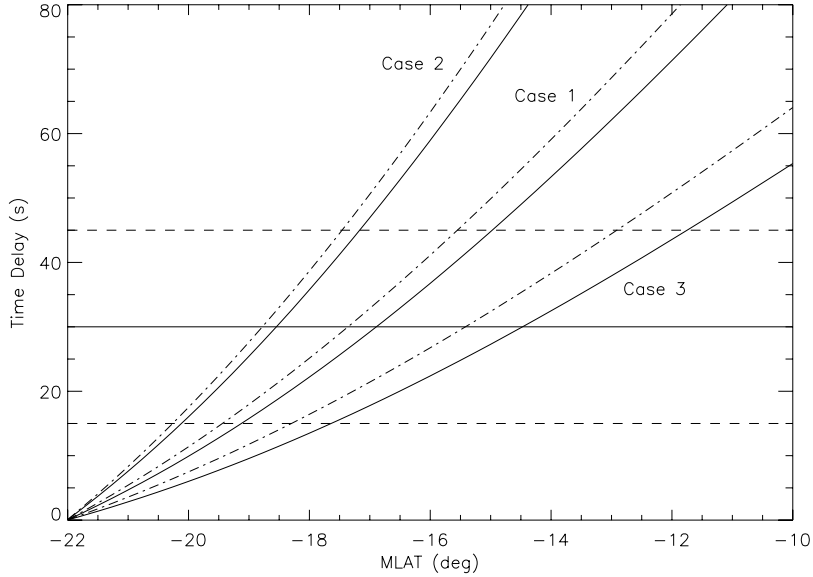

Figure 10. Assuming the ULF waves travel to Polar along B from some source closer to the equator at some MLAT, the curves give the time delay between the ULF wave transit time and the field-aligned proton travel time from the same source latitude to Polar's location at −22° MLAT. The two line styles correspond to two different proton energies (dash-dot 1 keV, solid 500 eV) and the three sets of curves correspond to cases described in the text.

value of α of ~1.7 was found for the plasmatrough by *Goldstein et al.* [2001].

[28] We note, however, that *Denton et al.* [2004] found that at $L \sim 7$ the mass density, as opposed to the electron density, was locally peaked at the magnetic equator, which may imply that in the plasmatrough heavy ions are preferentially concentrated at the magnetic equator. Similarly, *Takahashi et al.* [2004] found for $L > 6$ that the ratios of standing Alfven wave harmonics f_2/f_1 and f_3/f_1 did not fit a single value of α, which suggested again that the mass density did not follow a power law dependence. Their analysis also showed that the mass density was locally peaked at the magnetic equator, decreased off the equator, and then increased again at high latitude. Examination of Figure 12 of *Takahashi et al.* [2004] suggests that one might expect roughly equal mass densities at 0° and −27.5° MLAT, with approximately a 30% decrease at intervening latitudes. For this study we used three values of α, 0, −1, and 2. As Table 2 shows, variations in this parameter caused only minor changes in the local group velocity (compare cases 1, 6, and 7) and caused less than a 4% change in the calculated delay times.

[29] Because variations in α produced only relatively small variations in ion density along the field lines, the time delays for the nine cases shown in Table 2 can be described as falling into three ranges: (1) a low range associated with reduced He^+ densities or reduced total ion densities; (2) a middle range characterized by "typical" ion composition fractions, and for all tested values of α and η_O; and (3) a high range associated with doubled He^+ densities or doubled total ion densities.

[30] Figure 10 shows the time delays corresponding to cases 1, 2, and 3. The dash-dot line in each case corresponds to the time delay between waves and 1-keV ions, and the solid line corresponds to the delay between waves and 500-eV ions. In all cases, the delay times calculated assuming wave origin equatorward of −12° are significantly above the observed 30 ± 15 s time delay, and only for latitudes of −20° are they significantly below it. Given the uncertainty in our estimation technique and in the density models, we suggest based on the above modeling that the waves originated at −16° ± 4° MLAT. This result, suggesting that the waves were generated within 6° of Polar's location, conflicts with the common assumption that ion cyclotron waves are generated near the magnetic equator. Two factors, however, make this location reasonable. First, magnetic field lines in the daytime outer magnetosphere are known to be significantly nondipolar; the minimum magnetic field along Polar's field line according to the *Tsyganenko and Stern* [1996] field model was 172 nT, only 10% weaker than its value of 188 nT at −21.5°. Second, as shown in Figure 8, the "instability" parameter calculated according to *Gary et al.* [1995] was very near instability, so regions only slightly equatorward might well have been sufficiently unstable to generate the observed waves.

5. Summary

[31] This work has been an attempt to relate ground measurements of ULF waves made at multiple high-latitude sites with the Polar magnetometer measurements of ULF waves in the magnetosphere when the Polar spacecraft was in reasonable conjunction with the ground. It is well known that intensifications in ground dayside ULF wave power are often related to increases in the solar wind dynamic pressure. For the event studied, an abrupt solar wind pressure increase occurred after a period of relative quiet. The dynamic pressure of the solar wind never exceeded several nPa for a period of almost 13 days prior to the rapid increase to over 20 nPa on 18 March 2002. In addition to comparing

the Polar measurements of ULF waves in situ with the ground observations, a second objective was to use Polar Hydra energetic particle data and the Polar TIDE plasma data to evaluate whether the pressure induced modifications of these particles could be a local source of the waves via the instability driven by proton temperature anisotropy. A summary of the results of this work is as follows:

[32] 1. The pressure pulse created a significant population of protons between a few hundred eV and several keV mostly perpendicular to B. These protons seem to have replaced the quiescent stream of protons presumably from the plasma sheet that existed before the pressure pulse.

[33] 2. Following the pressure pulse, there was nearly a two order of magnitude increase in the population of thermal/superthermal (0.32–410 eV) protons measured by the TIDE instrument.

[34] 3. Cyclotron waves are expected to limit the proton temperature anisotropy $A = T_\perp/T_\parallel - 1$ roughly according to $A(\beta_{\parallel\ h})^{0.44}\ (n_c/n_h)^{0.25} \geq 0.5$ or as $A(\beta_{\parallel\ h})^{0.47} \geq 0.39$, where $\beta_{\parallel\ h}$ is the parallel plasma (proton) beta defined as $8\pi n_h k T_\parallel/B^2$.

[35] 4. In addition to the energization of protons transverse to B in the several keV range, the onset of lower energy protons (hundreds eV to few keV), predominantly aligned along B, play a significant role in whether the particle population is unstable at a given time by reducing the temperature anisotropy.

[36] 5. The Polar magnetometer measured in situ ULF waves during the entire time from pressure pulse onset to the time when Polar entered the magnetosheath. For the first 12 min of this time there was a combination of broadband waves and bandlimited Pc 1 displaying a great deal of structure and time variability. The instability calculation from the particle population using equation (1) showed that this could be a period of EMIC instability. After this period the ULF waves were more clearly bandwidth limited and correlated very well with the instability calculation using both equation (1) and equation (2); however, a 30–60 s delay in the measured ULF waves with respect to the calculated instability of the measured proton population was observed. It must be recognized that waves at Polar do not necessarily have to be generated at the position of Polar but could propagate from other sites along the field line. On the basis of the consistently poleward Poynting flux toward the Southern Hemisphere and numerical estimates based on the observed 30 ± 15 s delay from the observation of the particles to the observation of the waves, we infer that during the ULF wave burst at 1338 UT the origin of the waves was south of the magnetic equator and within 6° of Polar's location. This conflicts with the common assumption that ion cyclotron waves are generated near the equator. However, as shown in Figure 8, the ''instability'' parameter calculated according to *Gary et al.* [1995] was very near instability, so regions only slightly equatorward might well have been sufficiently unstable to generate the observed waves.

[37] 6. Ground ULF waves (classified as hydromagnetic chorus) were measured with varying clarity at five different ground sites, including SS in the Northern Hemisphere, from the onset of the pressure pulse for a duration of nearly an hour and a half, well after the time Polar entered the magnetosheath. The ground ULF data generally shows a great deal more structure than the Polar waves. Since the ground signals readily duct horizontally, it is quite likely the ground data represents ULF waves created on many different field lines. However, the most intense Polar ULF waves, between 1338 and 1345 UT (times when the calculated instability was the greatest) can be identified with the most intense ground ULF.

[38] **Acknowledgments.** This research was supported by National Science Foundation grants OPP-0233169 and OPP-0087317 to Augsburg College and by subcontracts to the University of New Hampshire and Dartmouth College from Augsburg College. The work at the U. of New Hampshire was additionally supported by a subcontract from Mission Research Corporation under NASA Contract NASW-01011. The Polar work at UCLA was supported by NASA grant NAG 5-11324. The Hydra particle measurements are supported at the U. of Iowa by NASA grant NAG 5-7883. The U. of New Hampshire Hydra work is supported by NASA grants NAG 5-13116 and NAG 5-11676. Work at Dartmouth was supported by NSF grant ATM-0245664. We acknowledge the assistance of the U. S. Antarctic Program in supporting the operation of search coil magnetometer at South Pole Station and of the British Antarctic Survey in supporting the operation of search coil magnetometers at the BAS AGOs.

[39] Lou-Chuang Lee thanks Robert Erlandson and Danny Summers for their assistance in evaluating this paper.

References

Anderson, B. J., and S. A. Fuselier (1993), Magnetic pulsations from 0.1 to 4.0 Hz and associated plasma properties in the Earth's subsolar magnetosheath and plasma depletion layer, *J. Geophys. Res.*, *98*, 1461–1479.

Anderson, B. J., and D. C. Hamilton (1993), Electromagnetic ion cyclotron waves stimulated by modest magnetospheric compressions, *J. Geophys. Res.*, *98*, 11,369–11,382.

Anderson, B. J., R. E. Erlandson, M. J. Engebretson, J. Alford, and R. L. Arnoldy (1996a), Source region of 0.2 to 1.0 Hz geomagnetic pulsation bursts, *Geophys. Res. Lett.*, *23*, 769–772.

Anderson, B. J., R. E. Denton, G. Ho, D. C. Hamilton, S. A. Fuselier, and R. J. Strangeway (1996b), Observational test of local proton cyclotron instability in the Earth's magnetosphere, *J. Geophys. Res.*, *101*, 21,527–21,543.

Anderson, H. M., M. J. Engebretson, R. L. Arnoldy, L. J. Cahill Jr., and P. T. Newell (1995), Statistical study of hydromagnetic chorus events at very high latitudes, *J. Geophys. Res.*, *100*, 3681–3692.

Bräysy, T., and K. Mursula (2001), Conjugate observations of electromagnetic ion cyclotron waves, *J. Geophys. Res.*, *106*, 6029–6041.

Denton, R. E., J. Goldstein, J. D. Menietti, and S. L. Young (2002), Magnetospheric electron density model inferred from Polar plasma wave data, *J. Geophys. Res.*, *107*(A11), 1386, doi:10.1029/2001JA009136.

Denton, R. E., K. Takahashi, R. R. Anderson, and M. P. Wuest (2004), Magnetospheric toroidal Alfven wave harmonics and the field line distribution of mass density, *J. Geophys. Res.*, *109*, A06202, doi:10.1029/2003JA010201.

Dudeney, J. R., R. B. Horne, M. J. Jarvis, R. I. Kressman, A. S. Rodger, and A. J. Smith (1997), British Antarctic Survey's ground-based activities complementary to satellite missions such as Cluster, in the *Satellite-Ground Based Coordination Sourcebook*, *ESA-SP-1198*, edited by M. Lockwood, M. N. Wild, and H. J. Opgenoorth, pp. 101–109, Eur. Space Agency Publ., Noordwijk, Netherlands.

Engebretson, M. J., et al. (1997), The United States automatic geophysical observatory (AGO) program in Antarctica, in the *Satellite-Ground Based Coordination Sourcebook*, *ESA-SP-1198*, edited by M. Lockwood, M. N. Wild, and H. J. Opgenoorth, pp. 65–99, Eur. Space Agency Publ., Noordwijk, Netherlands.

Engebretson, M. J., W. K. Peterson, J. L. Posch, M. R. Klatt, B. J. Anderson, C. T. Russell, H. J. Singer, R. L. Arnoldy, and H. Fukunishi (2002), Observatons of two types of Pc 1-2 pulsations in the outer dayside magnetosphere, *J. Geophys. Res.*, *107*(A12), 1451, doi:10.1029/2001JA000198.

Erlandson, R. E., L. J. Zanetti, M. J. Engebretson, R. Arnoldy, T. Bösinger, and K. Mursula (1994), Pc1 waves generated by a magnetospheric compression during the recovery phase of a geomagnetic storm, in *Solar Wind Sources of Magnetospheric Ultra-Low-Frequency Waves*, *Geophys. Monogr. Ser.*, vol. 81, edited by M. Engebretson, K. Takahashi, and M. Scholer, pp. 399–407, AGU, Washington, D. C.

Erlandson, R. E., K. Mursula, and T. Bösinger (1996), Simultaneous ground-satellite observations of structured Pc 1 pulsations, *J. Geophys. Res.*, *101*, 27,149–27,156.

Fukunishi, H., T. Toya, K. Koike, M. Kuwashima, and M. Kawamura (1981), Classification of hydromagnetic emissions based on frequency-time spectra, *J. Geophys. Res.*, *86*, 9029–9039.

Gary, S. P., M. B. Moldwin, M. F. Thomsen, D. Winske, and D. J. McComas (1994), Hot proton anisotropies and cool proton temperatures in the outer magnetosphere, *J. Geophys. Res*, *99*, 23,603–23,615.

Gary, S. P., M. F. Thomsen, L. Yin, and D. Winske (1995), Electromagnetic proton cyclotron instability: Interactions with magnetospheric protons, *J. Geophys. Res*, *100*, 21,961–21,972.

Goldstein, J., R. E. Denton, M. K. Hudson, E. G. Miftakhova, S. L. Young, J. D. Menietti, and D. L. Gallagher (2001), Latitudinal density dependence of magnetic field lines inferred from polar plasma wave data, *J. Geophys. Res.*, *106*, 6195–6201.

Guglielmi, A., J. Kangas, and A. Potapov (2001), Quasiperiodic modulation of the Pc 1 geomagnetic pulsations: An unsettled problem, *J. Geophys. Res.*, *106*, 25,847–25,855.

Harvey, P., et al. (1995), The electric field instrument on the Polar spacecraft, *Space Sci. Rev.*, *71*, 583–596.

Heacock, R. R., and V. P. Hessler (1965), Pearl-type micropulsations associated with magnetic storm sudden commencements, *J. Geophys. Res.*, *70*, 1103–1111.

Hirasawa, T. (1981), Effects of magnetospheric compression and expansion on spectra structure of ULF emissions, paper presented at Third Symposium on Coordinate Observations of the Ionosphere and Magnetosphere in the Polar Regions, Natl. Inst. Polar Res., Tokyo.

Jacobs, J. A., and T. Watanabe (1963), Trapped charged particles as the origin of short period geomagnetic pulsations, *Planet. Space Sci.*, *11*, 869–878.

Jordanova, V. K., C. J. Farrugia, R. M. Thorne, G. V. Khazanov, G. D. Reeves, and M. F. Thomsen (2001), Modeling ring current proton precipitation by electromagnetic ion cyclotron waves during the May 14–16, 1997, storm, *J. Geophys. Res.*, *106*, 7–22.

Kokubun, S., and T. Oguti (1968), Hydromagnetic emissions associated with storm sudden commencements, *Rep. Ionosph. Space Res. Jpn.*, *22*, 45.

Kozyra, J. U., V. K. Jordanova, R. B. Horne, and R. M. Thorne (1997), Modeling of the contribution of electromagnetic ion cyclotron (EMIC) waves to stormtime ring current erosion, in *Magnetic Storms*, *Geophys. Monogr. Ser.*, vol. 98, edited by B. T. Tsurutani et al., pp. 187–202, AGU, Washington, D. C.

Lepping, R. P., et al. (1995), The Wind Magnetic Field Investigation, *Space Sci. Rev.*, *71*, 207–229.

Lu, G., T. G. Onsager, G. Le, and C. T. Russell (2004), Ion injections and magnetic field oscillations near the high-latitude magnetopause associated with solar wind dynamic pressure enhancements, *J. Geophys. Res.*, *109*, A06208, doi:10.1029/2003JA010297.

Menk, F. W., B. J. Fraser, H. J. Hansen, P. T. Newell, C.-I. Meng, and R. J. Morris (1993), Multistation observations of Pc1-2 ULF pulsations in the vicinity of the polar cusp, *J. Geomagn. Geoelectr.*, *45*, 1159–1173.

Moore, T. E., et al. (1995), The Thermal Ion Dynamics Explorer and Plasma Source Instrument, *Space Sci. Rev.*, *71*, 409–458.

Mursula, K., R. Rasinkangas, and T. Bösinger (1997), Nonbouncing Pc 1 wave bursts, *J. Geophys. Res.*, *102*, 17,611–17,624.

Mursula, K. T. Bräysy, K. Niskala, and C. T. Russell (2001), Pc1 pearls revisited: Structured electromagnetic ion cyclotron waves on Polar satellite and on the ground, *J. Geophys. Res.*, *106*, 29,543–29,533.

Ogilvie, K. W., et al. (1995), A comprehensive plasma instrument for the Wind spacecraft, *Space Sci. Rev.*, *71*, 55–77.

Olson, J. V., and L. C. Lee (1983), Pc 1 wave generation by sudden impulses, *Space Sci.*, *31*, 295–296.

Quinn, J. M., and D. J. Southwood (1982), Observations of parallel ion energization in the equatorial region, *J. Geophys. Res.*, *87*, 10,536–10,540.

Rosenberg, T. J., and J. H. Doolittle (1994), Studying the polar ionosphere and magnetosphere with Automatic Geophysical Observatories: The United States program in Antarctica, *Antarctic J. U. S.*, *29*(5), 347–349.

Russell, C. T., R. C. Snare, J. D. Means, D. Pierce, D. Dearborn, M. Larson, G. Barr, and G. Le (1995), The GGS Polar magnetic field investigation, *Space Sci. Rev.*, *71*, 563–582.

Scudder, J. D., et al. (1995), Hydra – A 3-dimensional electron and ion hot plasma instrument for the POLAR spacecraft of the GGS mission, *Space Sci. Rev.*, *71*, 459–495.

Song, P., R. C. Elphic, C. T. Russell, J. T. Gosling, and C. A. Cattell (1990), Structure and properties of the subsolar magnetopauses for northward IMF: ISEE observations, *J. Geophys. Res.*, *95*, 6375–6387.

Summers, D., and R. M. Thorne (2003), Relativistic electron pitch-angle scattering by electromagnetic ion cyclotron waves during geomagnetic storms, *J. Geophys. Res.*, *108*(A4), 1143, doi:10.1029/2002JA009489.

Takahashi, K., R. E. Denton, R. R. Anderson, and W. J. Hughes (2004), Frequencies of standing Alfven waves harmonics and their implication for plasma mass distribution along geomagnetic field lines: Statistical analysis of CRRES data, *J. Geophys. Res.*, *109*, A08202, doi:10.1029/2003JA010345.

Taylor, W. W. L., B. K. Parady, P. B. Lewis, R. L. Arnoldy, and L. J. Cahill Jr. (1975), Initial results from the search coil magnetometer at Siple, Antarctica, *J. Geophys. Res.*, *80*, 4762–4769.

Thorne, R. M., and R. B. Horne (1994), Energy transfer between energetic ring current H^+ and O^+ by electromagnetic ion cyclotron waves, *J. Geophys. Res.*, *99*, 17,275–17,282.

Thorne, R. M., and R. B. Horne (1997), Modulation of electromagnetic ion cyclotron instability due to interaction with ring current O+ during magnetic storms, *J. Geophys. Res.*, *102*, 14,155–14,163.

Troitskaya, V. A. (1961), Pulsations of the earth's electromagnetic field with periods of 1 to 1.5 seconds and their connection with phenomena in the high atmosphere, *J. Geophys. Res.*, *66*, 5–18.

Troitskaya, V. A., E. T. Matveyeva, K. G. Ivanov, and A. V. Gul'yelmi (1968), Change in the frequency of Pc1 micropulsations during a sudden deformation of the magnetosphere, *Geomagn. Aeron.*, *8*, 784.

Tsurutani, B. T., G. S. Lakhina, L. Zhang, J. S. Pickett, and Y. Kasahara (2003), ELF/VLF plasma waves in the low latitude boundary layer, in *Earth's Low-Latitude Boundary Layer*, *Geophys. Monogr. Ser.*, vol. 133, edited by P. T. Newell and T. Onsager, pp. 189–203, AGU, Washington, D. C.

Tsyganenko, N. A. (1989), Magnetospheric magnetic field model with a warped tail current sheet, *Planet. Space Sci.*, *37*, 5.

Tsyganenko, N. A., and D. P. Stern (1996), Modeling the global magnetic field of the large-scale Birkeland current system, *J. Geophys. Res.*, *101*, 27,187–27,198.

R. L. Arnoldy, C. F. Farrugia, M. R. Lessard, and R. B. Torbert, University of New Hampshire, Durham, NH 03824, USA. (roger.arnoldy@unh.edu; charlie.farrugia@unh.edu; marc.lessard@unh.edu; roy.torbert@unh.edu)

S.-H. Chen and T. E. Moore, NASA Goddard Space Flight Center, Greenbelt, MD 20771, USA. (sheng-hsien.chen@gsfc.nasa.gov; thomas.e.moore@nasa.gov)

R. E. Denton, Dartmouth College, Hanover, NH 03755, USA. (richard.e.denton@dartmouth.edu)

M. J. Engebretson and J. L. Posch, Augsburg College, Minneapolis, MN 55454, USA. (engebret@augsburg.edu; posch@augsburg.edu)

N. C. Maynard and D. M. Ober, ATK Mission Research, Nashua, NH 03062, USA. (nelson.maynard@atk.com; dan.ober@atk.com)

C. T. Russell, Institute of Geophysics and Planetary Physics, University of California, Los Angeles, CA 90095, USA. (ctrussell@igpp.ucla.edu)

J. D. Scudder, University of Iowa, Iowa City, IA 52242, USA. (jds@space-theory.physics.uiowa.edu)